Electromagnetic transmission in configurations composed of two one-dimensional perfect electric conductor metal gratings

Ji Xu (许 吉)[1], Chen Cheng (程 晨)[1], Zhu Zheng (郑 渚)[1], Jing Chen (陈 璟)[2], Qiang Bai (白 强)[1], Cong Liu (刘 聪)[1], and Huitian Wang (王慧田)[1,2*]

[1]*National Laboratory of Solid State Microstructures and Department of Physics, Nanjing University, Nanjing 210093, China*

[2]*School of Physics and Key Laboratory of Weak Light Nonlinear Photonics, Nankai University, Tianjin 300071, China*

[*]*E-mail: htwang@nju.edu.cn*

Received March 23, 2010

We study transmission properties in configurations composed of two single metal gratings with different thicknesses. Choosing the perfect electric conductor excludes the influence of intrinsic material dispersion on transmission behaviors; and as such, we aim to reveal the contribution of geometric dispersion to electromagnetic transmission. Transmission suppression line, instead of a transmission suppression point, is discovered, denoting the curve of the wavelength versus the interval or the lateral displacement between the two single gratings when the transmission suppression appears. A simplified model is proposed to comprehend the underlying physics of this special phenomenon.

OCIS codes: 260.2110, 050.2770, 120.7000.
doi: 10.3788/COL20100808.0807.

Due to the unique properties of extraordinary electromagnetic (EM) transmission[1], subwavelength metal microstructures[2−8] have been used in numerous important applications in various fields[9,10]. However, most published works have focused on single-metal slabs with subwavelength microstructures, i.e., single-metal grating (SMG). Few studies have focused on configurations consisting of two or more metal gratings[11−13]. Recently, we have shown that a dual-metal grating (DMG) structure composed of two identical SMGs exhibits some interesting EM properties[14,15], such as controllable EM transmission. The dispersion of metal obeys the Drude model. Intrinsic and geometric dispersions coexist; hence, it is difficult to distinguish their individual contributions to EM transmission. In this letter, we choose a metal as the perfect electric conductor (PEC) with permittivity $\varepsilon_{\rm m} \to -\infty$ in order to exclude the contribution of intrinsic material dispersion.

We deal with the PEC DMG structure composed of two PEC SMGs with different thicknesses. We discover the presence of transmission suppression (TS, zero transmission) line, instead of a transmission suppression point[14,15]. The TS line denotes the curve of the zero-transmission wavelength versus the gap or the lateral displacement between the two single gratings. A simplified model is proposed to comprehend the underlying physics of this special phenomenon.

The treated PEC DMG structure and its geometric parameters are shown in Fig. 1. Different from Refs. [14,15], the two PEC SMGs can have different thicknesses of h_1 and h_2. The slit width in any PEC SMG is fixed at $a = 0.100\ d$.

We first investigated the dependence of the transmission spectrum of the PEC SMG on the grating thickness. The results validate that at a chosen transmission peak (TP) wavelength, such as $\lambda = 1.500\ d$, the required grating thickness is $h = m\lambda/2 + 0.600\ d$ (m is an integer, $m \geq 0$). This implies that the difference in the required grating thickness is the integral multiple of a half wavelength. It should be pointed out that the two end faces of the slit offer additional phases of reflection[6], which explains why the SMG thickness of the 0th-order Fabry-Pérot-like (F-P-like) mode is not a half wavelength.

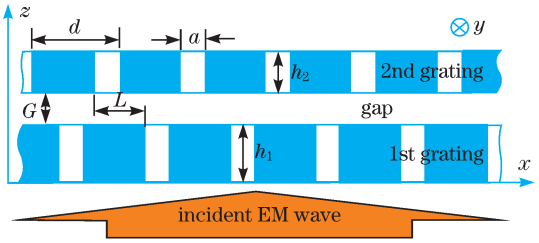

Fig. 1. Scheme of PEC DMG structure and its geometric parameters.

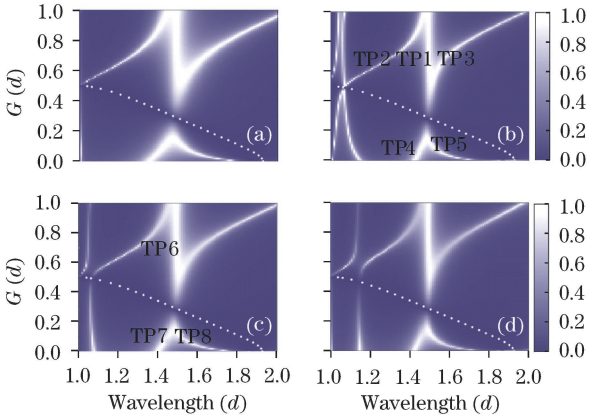

Fig. 2. Dependence of transmission spectrum on G when $L = 0$ in the DMG structure. (a) $h_1 = h_2 = 0.600\ d$; (b) $h_1 = h_2 = 1.350\ d$; (C) $h_1 = 0.600\ d$, $h_2 = 1.350\ d$; (d) $h_1 = 0.600\ d$, $h_2 = 2.100\ d$. The dotted lines are the curves calculated by Eq. (3).

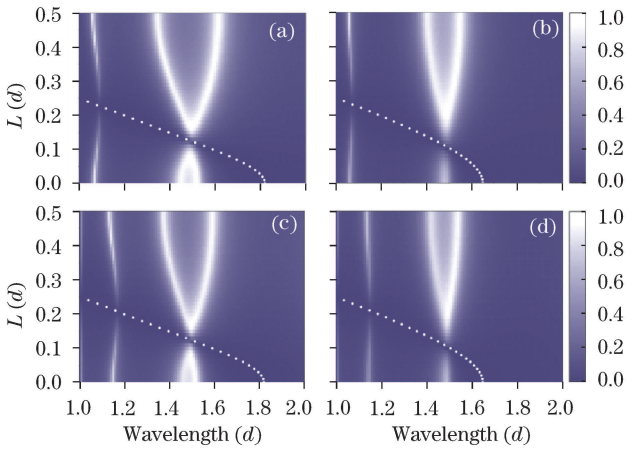

Fig. 3. Dependence of the transmission spectrum on L in the DMG structure. The left and right columns correspond to G = 0.100 d and G = 0.200 d, respectively. (a), (b) h_1 = 0.600 d, h_2 = 1.350 d; (c), (d) h_1 = 0.600 d, h_2 = 2.100 d. The dotted lines are the curves calculated using Eq. (3).

To construct the PEC DMG structures, we chose two PEC SMGs to support TP at the same wavelength (λ = 1.500 d), indicating that h_1 and h_2 should be $m\lambda/2$ + 0.600 d. Figure 2 shows the dependence of the calculated transmission spectra on the gap G between two gratings, without the lateral shift (L = 0). On the other hand, Fig. 3 displays the influences of L on the transmission spectra when G = 0.100 d and 0.200 d.

From Figs. 2 and 3, we obtain four conclusions as follows. (i) There always exists a TP located at the wavelength λ =1.500 d above the TS line. (ii) When G becomes small, a single TP splits into two TPs below the TS line. (iii) There occurs a TS line (which embodies the curve of the zero-transmission wavelength λ versus G or L), instead of a single TS point in Ref. [15]. (iv) The TS line is determined only by G, L, and λ, and it is independent of the grating thicknesses of two PEC SMGs within a fixed period.

To further understand the transmission property in the PEC DMG structure, we provide an example that focuses on the transmission spectrum of the PEC DMG with h_1 = h_2 = 1.350 d (Fig. 2(b), where five TPs of great interest are labeled). According to different properties, they can be classified into three groups: TP1, TP2 and TP3, and TP4 and TP5. Groups (TP1) and (TP2 and TP3) correspond to the large gap (G = 0.700 d), while group (TP4 and TP5) corresponds to the small gap (G = 0.100 d). The **H** field distributions at these TPs are depicted in Fig. 4.

TP1 (1.500 d, 0.700 d) in the PEC DMG has the same transmission wavelength as the PEC SMG with the thickness of 1.350 d. The **H** field distribution of TP1 exhibits no resonance or interference in the gap, and has a typical profile of F-P-like resonance in the slits. This indicates that the interaction between the two SMGs has no influence on the F-P-like mode in the PEC SMG, and TP1 originates from the cascaded transmission of the two PEC SMGs. TP2 (1.313 d, 0.700 d) and TP3 (1.585 d, 0.700 d) have a common feature: the **H** field exhibits the F-P-like resonance with a node along the z direction in the gap, but there is no F-P-like resonance in the slits. Therefore, TP2

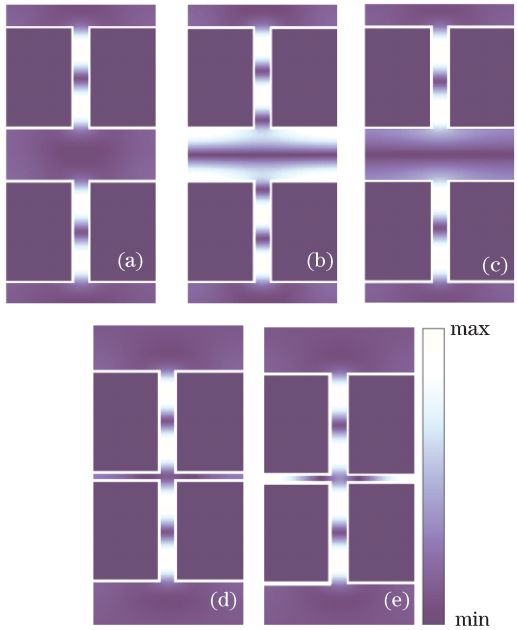

Fig. 4. **H** field distributions at five TPs. (a) TP1, λ = 1.500 d; (b) TP2, λ = 1.313 d; (c) TP3, λ = 1.585 d; (d) TP4, λ = 1.465 d; (e) TP5, λ = 1.518 d.

and TP3 should be from the F-P-like resonance caused by the coupling between the two PEC SMGs. TP4 (1.465 d, 0.100 d) and TP5 (1.518 d, 0.100 d), as a pair of twinborn TPs, are from the splitting of the single TP at λ = 1.500 d, and are the result of the coupling between two PEC SMGs. As G decreases, the coupling between the two PEC SMGs becomes stronger; in turn, this enlarges the interval between the twinborn TPs. When the gap is reduced to G = 0, the strongest coupling occurs, and the single TP is split into a pair of twinborn TPs at the wavelengths of λ = 1.428 d and 1.854 d. These are just the 3rd- and 2nd-order F-P-like modes in the PEC SMG with the thickness of 2.700 d, respectively. Different from the three TPs (TP1, TP2, and TP3), **H** field distributions at TP4 and TP5 exhibit the interference pattern in the x direction in the gap. It implies that, in the case of small G, the high-order evanescent diffracted modes in the gap have the dominant contribution to the coupling between the two PEC SMGs, resulting in the splitting of TP.

We also explore the situation of the two PEC SMGs with different thicknesses as h_1 = 0.600 d and h_2 = 1.350 d . The calculated **H** field distributions at TP6, TP7, and TP8 labeled in Fig. 2(c) are not shown here. Meanwhile, TP6 (1.500 d, 0.700 d) is similar to TP1, originating from the cascaded transmission of two PEC SMGs. However, the F-P-like resonances in the two SMGs have different orders. The **H** field distributions of TP7 (1.450 d, 0.100 d) and TP8 (1.520 d, 0.100 d) exhibit the same interference patterns in the gap as those of TP3 and TP4. In fact, they are also a pair of twinborn TPs resulting from the coupling between F-P-like resonances of different orders. In particular, we can see the existence of the TS line, instead of a TS point. The TPs above the TS line have a completely different mechanism from the TPs below the TS line.

The TS line is independent of the thicknesses of the

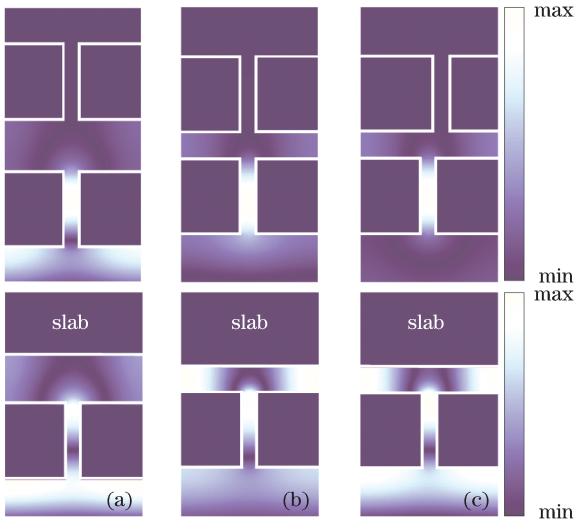

Fig. 5. **H** field distributions when TS occurs in the DMG structure composed with SMGs of $h_1 = h_2 = 0.600\ d$ and in the SMG/slab simplified structure. (a) $G = 0.400\ d$, $L = 0$, and $\lambda = 1.280\ d$; (b) $G = 0.200\ d$, $L = 0$, and $\lambda = 1.630\ d$; (c) $G = 0.200\ d$, $L = 0.097\ d$, and $\lambda = 1.500\ d$.

two PEC SMGs; hence, it can be asserted that the TS phenomenon is not related to the F-P-like resonance in the slits, and only depends on diffracted modes from the slits in the gap. The foregoing discussions regarding the TPs suggest that the TS line is a watershed (or a division) separating the two regimes. In the regime above the TS line (i.e., corresponding to the case of the larger gap G), the 0th-order diffracted mode in the gap dominates the interaction between the two SMGs. In contrast, in the regime below the TS line (i.e., corresponding to the case of the smaller gap G), the higher order diffracted evanescent modes in the gap govern the coupling of the two SMGs.

The contour maps in the upper row of Fig. 5 show the calculated **H** field distributions at some points in the TS line. From these, some common features may be observed. For example, in the 2nd SMG, there is almost no EM field in the slits and at the entrances of slits. Hence, the 2nd SMG can be considered to be a uniform PEC slab, implying that the PEC DMG structure can be degenerated to the SMG/slab configuration. Based on this simplified structure, the recalculated **H** field distributions are shown by the contour maps in the bottom row of Fig. 5. A comparison between the true and simplified structures shows that the **H** field distributions in the gap are quite similar, and that the regions of zero **H** field are almost the same. We assert that the presence of the TS phenomenon originates from the zero **H** field at the entrance of the slit in the 2nd PEC SMG. The F-P-like resonances in the slits in the 1st PEC SMG have almost no influence on the TS behavior; hence, the 1st SMG can also be treated as a PEC slab. In particular, EM transmission through the 1st SMG can be simplified into a one-dimensional (1D) periodic array of line radiation sources located at the exits of the slits on the back surface of the 1st SMG, with a period of d. When the line source is located at the center of a period, the periodic boundary continuity condition can be replaced by the PEC boundary condition. Finally, the DMG structure is simplified to an enclosed rectangular PEC cavity with the dimensions of $G \times d$ having a line source located at the middle of the bottom side with a width d.

Based on the foregoing simplified model, the problem becomes the following Helmholtz equation for the **H** field component H_y:

$$\left[\frac{\partial^2}{\partial x^2} + \frac{\partial^2}{\partial y^2} + k^2\right] H_y(x,z) = \delta(x,z)\big|_{x=d/2,z=0}, \quad (1)$$

where $k{=}2\pi/\lambda$. Using $\nabla \times \mathbf{H} = \varepsilon_0 \partial \mathbf{E}/\partial t$ and under the EM boundary conditions, the solution of H_y is expressed as

$$H_y(x,z) = \frac{4}{dG} \sum_{m,n=-\infty}^{\infty} \frac{\cos(k_x x)\cos(k_x d/2)\cos(k_z z)}{k^2 - k_x^2 - k_z^2}, \quad (2)$$

where $k_x = m\pi/d$, $k_z = n\pi/G$, m and n are two integers. When the TS phenomenon occurs, the entrance of any slit in the 2nd SMG feels a zero field. The TS line can then be given as

$$H_y(x_0, G) = 0, \quad (3)$$

where $x_0 = d/2{-}L$. Evidently, the solution depends on three geometric parameters (i.e., G, d, and L) and the wavelength λ. For the various situations shown in Figs. 2 and 3, the numerically calculated TS lines by Eq. (3) are depicted by the dotted lines that are in good agreement with the TS lines observed in the simulated transmission spectra. Certainly, there still exists a little imprecision when G is small. We believe this is primarily caused by the line source approximation.

In conclusion, the simulated transmission spectra show the existence of the TS line, instead of a single TS point. It should be emphasized that the TS phenomenon is a common and universal feature of DMG structures. The TS phenomenon originates from the zero fields at the entrances of the slits in the 2nd SMG. This phenomenon is caused by destructive interference among high-order evanescent modes diffracted by the exits of the slits in the 1st SMG. We develop a simplified model to comprehend the underlying physics of the TS phenomenon. The TS line predicted from our simplified model is in good agreement with the simulated transmission spectra.

This work was supported by the National Natural Science Foundation of China (No. 10974102) and the National Basic Research Program of China (No. 2006CB921805).

References

1. T. W. Ebbesen, H. J. Lezec, H. F. Ghaemi, T. Thio, and P. A. Wolff, Nature **391,** 667 (1998).
2. K. J. K. Koerkamp, S. Enoch, F. B. Segerink, N. F. van Hulst, and L. Kuipers, Phys. Rev. Lett. **92,** 183901 (2004).
3. J. A. Porto, F. J. García-Vidal, and J. B. Pendry, Phys. Rev. Lett. **83,** 2845 (1999).
4. Q. Cao and P. Lalanne, Phys. Rev. Lett. **88,** 057403 (2002).
5. H. J. Lezec, A. Degiron, E. Devaux, R. A. Linke, L. Martin-Moreno, F. J. Garcia-Vidal, and T. W. Ebbesen, Science **297,** 820 (2002).
6. Y. Takakura, Phys. Rev. Lett. **86,** 5601 (2001).

7. L. Wang, K. Xia, H. Sun, Y. Niu, and S. Gong, Chin. Opt. Lett. **5,** S126 (2007).
8. X. Yang and D. Liu, Chin. Opt. Lett. **5,** 563 (2007).
9. W. L. Barnes, A. Dereux, and T. W. Ebbesen, Nature **424,** 824 (2003).
10. E. Altewischer, M. P. van Exter, and J. P. Woerdman, Nature **418,** 304 (2002).
11. J. T. Shen and P. M. Platzman, Phys. Rev. B **70,** 035101 (2004).
12. H. B. Chan, Z. Marcet, K. Woo, D. B. Tanner, D. W. Carr, J. E. Bower, R. A. Cirelli, E. Ferry, F. Klemens, J. Miner, C. S. Pai, and J. A. Taylor, Opt. Lett. **31,** 516 (2006).
13. G. Xiao, X. Yao, X. Ji, J. Zhou, Z. Bao, and Y. Huang, Chin. Opt. Lett. **6,** 791 (2008).
14. C. Cheng, J. Chen, Q.-Y. Wu, F.-F. Ren, J. Xu, Y.-X. Fan, and H.-T. Wang, Appl. Phys. Lett. **91,** 111111 (2007).
15. C. Cheng, J. Chen, D.-J. Shi, Q.-Y. Wu, F.-F. Ren, J. Xu, Y.-X. Fan, J. Ding, and H.-T. Wang, Phys. Rev. B **78,** 075406 (2008).